Publications

Available Online

J. Sci. Res. **14** (1), 101-114 (2022)

JOURNAL OF SCIENTIFIC RESEARCH

www.banglajol.info/index.php/JSR

Investigation of Fibrous Materials for Low Frequency and High-Frequency Passive Noise Reduction using Transfer Matrix Method

R. Sreeja[1,2*]

[1]Maharajas College (A Government Autonomous College), Ernakulam, Kerala, India 682011

[2]University of Kerala, Thiruvananthapuram, Kerala, India 695034

Received 22 May 2021, accepted in final revised form 18 September 2021

Abstract

The concern about the adverse effects of noise pollution is enhancing day by day due to fast industrialization. Hence a wide variety of active and passive noise controllers made of natural and synthetic materials are widely used for various types of inevitable noise reduction. The different types of passive noise controllers fabricated using various techniques vary in their microstructure and surface morphology. In turn, they cause a difference in the noise-controlling mechanisms happening inside it, leading to its unique acoustic absorption characteristics. This article uses five different fibers of different fiber diameters to fabricate passive acoustic absorbers of different textures. The frequency response of their acoustic absorption coefficient is tested with the help of impedance tube apparatus using the transfer matrix method. Acoustic properties of coir fiber, basalt fiber, glass fiber, graphene fiber, and carbon fiber are investigated and compared. The present investigation focused on the influence of fiber diameter, the porosity, and the difference in the texture of these passive absorbers on the acoustic characteristics, frequency response of acoustic absorption coefficient, and the frequency corresponding to maximum absorption. The investigation also focuses on fabricating the passive absorbers for low-frequency noise reduction where only the active absorbers are available.

Keywords: Acoustic absorption coefficient; Impedance tube; Transfer matrix; Passive acoustic absorber.

doi: http://dx.doi.org/10.3329/jsr.v14i1.53546 J. Sci. Res. **14** (1), 101-114 (2022)

1. Introduction

Fast industrialization and technological leaps create severe noise pollution all over the world. The ecosystem involving wildlife, aquatic life, and human life is under the threat of noise pollution, which adversely affects physical cum mental health and reproduction in various ways [1-12]. Due to these emerging environmental and health concerns, passive noise controlling techniques are getting prominence. Different types of linear and nonlinear single-channel and multi-channel active noise controllers are widely used in the various frequency regions for noise reduction purposes [13]. Electroacoustic,

* *Corresponding author*: sreeja.prasanth@gmail.com

piezoelectric, and hybrid active noise controllers are commonly used for noise and vibration control in the motor vehicle interiors for passenger comfort with a vibration-free interior of low noise pollution. It is also used for noise and vibration control in advanced instruments to reduce the wear and tear produced by the unwanted noise and vibration, which adversely affect the efficiency of the performance of sophisticated parts of these machines. Active noise controllers are proven efficient in noise controlling in the low-frequency region, whereas passive ones are less efficient. Despite all these advantages, these active noise controllers are less energy-efficient than the passive ones as they need external power for their functioning. In contrast, the other one's functions without external energy sources [14-16]. Different types of natural and synthetic passive acoustic absorbers are also widely used in a wide variety of noise reduction applications. Their structural and morphological difference affects the noise-controlling mechanisms and introduces a difference in their noise handling performance. The material's phonon dispersion and microstructural configuration are prominent in determining its acoustic properties [17]. Fibrous, granular, and tubular structured passive absorbers are typical of this kind [18-22]. The micro-perforated panel absorbers and slotted absorbers are used in passive absorption as their geometrical parameters can be optimized correctly in a suitable combination for the best noise controlling performance through proper modeling. This study investigates natural fiber-based passive acoustic absorbers for their acoustic characteristics even though micro-perforated panel absorbers, Helmholtz resonators, and Acoustic Meta Materials are proven efficient in absorbing acoustic fields low frequency as well as a high-frequency region [23-25]. Natural fiber-based passive acoustic absorbers are developed for high frequency and low-frequency noise reduction applications as they are eco-friendly and biodegradable compared to synthetic ones. The structural difference, fiber diameter, and texture can introduce drastic differences in passive noise control performance and the frequency in which it absorbs maximum sound energy. The frequency response of the acoustic absorption coefficient also varies according to the above criteria [26,27]. In this article, it is tried to investigate the influence of the standards mentioned above on the acoustic absorption performance and the frequency response of the acoustic absorption coefficient of the passive absorbers made of five different potential fibers, namely coir fiber, glass fiber, basalt fiber, carbon fiber, and graphene fiber. The coir fibers of three different fiber diameters of 120, 180, and 200 μm are used in this study to make passive absorbers in the form of pellets to understand the influence of fiber diameter on acoustic absorption performance. The frequency response of the coir mats of three different weaving patterns is recorded. The glass fiber, basalt fiber, carbon fiber, and graphene fiber-based epoxy laminates are fabricated with the Vacuum Assisted Resin Transfer Molding (VARTM) technique and investigated for acoustic frequency response. All the studies are carried out in an impedance tube apparatus with four microphones. The present investigation mainly concentrates on optimizing the passive fiber-based acoustic absorbers for low-frequency noise controlling. The fiber diameter's effect, nature of the material, and its texture on acoustic absorption property are also established through this study.

2. Fabrication of the Samples

The fiber materials used as the main constituent in this study for preparing the samples as passive noise controllers include coir fiber, glass fiber, basalt fiber, carbon fiber, and graphene fiber. Coir fiber is used in two different textures: the pelletized form and coir mats of varying weaving patterns. The fibers of other ones are used in the form of an epoxy laminate form prepared using the VARTM technique [28]. The coir fibers of three different fiber diameters, namely 120, 180, and 200 µm, are used in this present study for preparing the pellets. The samples are crafted in a pelletizer to get cylindrical-shaped coir pellets of 5 cm diameter of the same thickness. In this study Epoxy LY556 mixed with hardener HY951 by 10 % weight is used as the binder. Commercially available coir mats of three different weaving patterns, namely Panama weaved, Herringbone weaved, and Boucle weaved, are used in this investigation. The glass fiber, basalt fiber, carbon fiber, and graphene fiber-based epoxy laminates are prepared using VARTM. The fiber mats of these materials are used here for the sample preparation. The cleaning of the mold surface is done with the help of Acetone. For the easy removal of the sample, coating wax is applied to the clean and dry mold surface. Sixteen layers of mats of basalt fibers weighing 384 g are used for preparing the basalt composite, and the sealant tape is placed on the surface. Epoxy LY556 is mixed with hardener HY951 in the ratio 10:1. The spiral tube is fitted to a Vacuum pump used to vacuum out the system's air after placing the peel ply, distribution mesh, and vacuum bag correctly so that there should be no leakage of vacuum. Vacuum-infusion assisted hand lay-up method is used here. It offers more benefits than the hand lay-up method due to the better fibers to resin bonding resulting in more robust and lighter laminates. Fig. 1 shows the schematic diagram of the VARTM setup. The glass fiber, carbon fiber, and graphene fiber-based epoxy laminates used in this study are also fabricated in the same manner using the commercially available fiber sheets of the same. The prepared samples are taken out carefully and cut into circular-shaped pieces of 5 cm diameter for placing in the sample holder of the impedance tube apparatus for acoustic characterization.

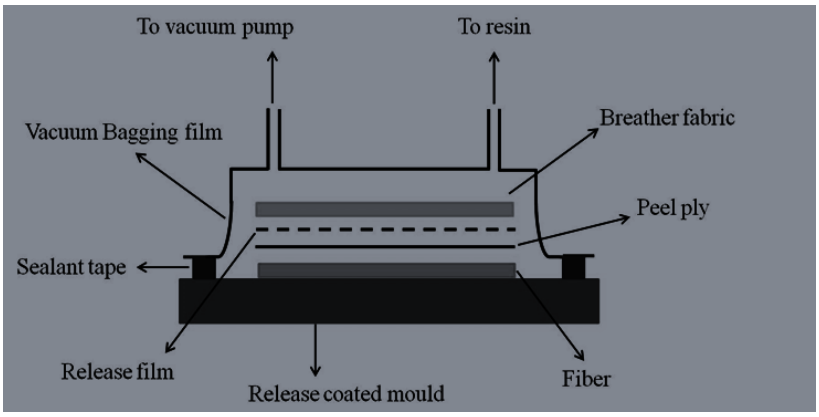

Fig. 1. Schematic diagram of the VARTM setup.

3. Experimental Setup Used for Acoustic Characterization

Four microphone impedance tube is used for characterizing the sample. The schematic diagram of the experimental setup used in this particular investigation is sown in Fig. 2.

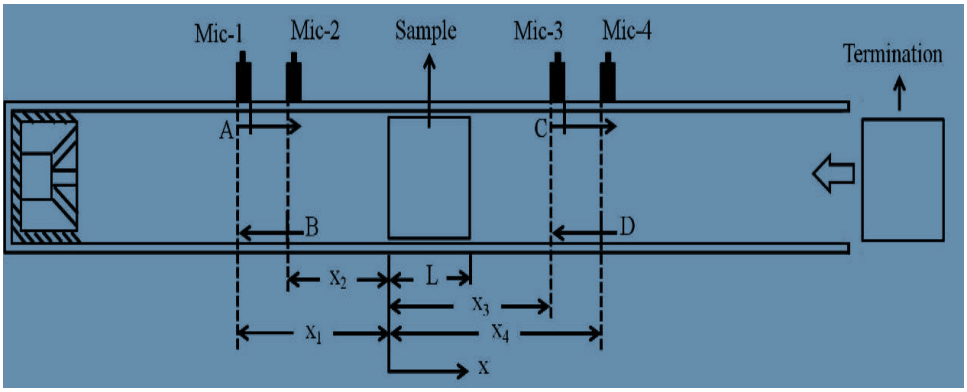

Fig. 2. Schematic diagram of the impedance tube set up used for acoustic characterization.

The material sample whose acoustic characterization is to be done is placed in the sample holding unit at the middle portion of the tube. The sound signals in the desired frequency region entering the sample are detected and measured at two positions. Similarly, the sound signals after entering the sample are also recorded at two positions. The recording is done with the help of a four-microphone impedance tube. The two microphones are placed on the input (m_1 and m_2) and the sample's output side (m_3 and m_4). These signals are correctly solved for calculating the pressure and velocity of the acoustic field at the incident side (x=0) and transmitted side (x=d) of the sample of thickness d. The acoustic field's sound pressure levels and velocity at x=0 and x=d are related through the transfer matrix T with elements T_{11}, T_{12}, T_{21}, and T_{22}. The signal's amplitude components at the incident side of the sample A and B in terms of the signals p_1 and p_2 at microphones m_1 and m_2 are given in equations (1) and (2). The amplitude components of the signal in the transmitted side of the sample C and D in terms of the signals p_3 and p_4 at microphones m_3 and m_4 are given in equations (3) and (4). The sound pressure and velocity on the incident side of the sample and the transmitted side of the sample at x=0 and x=d is given equation (5) and (6). The sound pressure and velocity on the incident side of the sample and the transmitted side of the sample in terms of the transfer matrix and the transfer matrix elements are given in equation (7) and equation (8), respectively. The acoustic parameters of the specimen under test are evaluated using the transfer matrix elements with the known values of density of the medium ρ and the sound velocity c. The acoustic reflection coefficient R and the absorption coefficient α of the sample in terms of the transfer matrix elements are shown in equations (9 and 10) [26,27]. The experiment is conducted for all the samples under investigation, namely coir pellets with three different fiber diameters, coir mats of three different weaving patterns of different selected

thicknesses, glass fiber epoxy laminate, basalt fiber epoxy laminate, carbon fiber epoxy laminate, and graphene epoxy laminate. In each case, the frequency response of the acoustic absorption coefficient is measured for analysis in the desired frequency range.

$$A = \frac{j\left(P_1 e^{jkx_2} - P_2 e^{jkx_1}\right)}{2\sin k(x_1 - x_2)} \tag{1}$$

$$B = \frac{j\left(P_2 e^{jkx_1} - P_1 e^{-jkx_2}\right)}{2\sin k(x_1 - x_2)} \tag{2}$$

$$C = \frac{j\left(P_3 e^{jkx_4} - P_4 e^{jkx_3}\right)}{2\sin k(x_3 - x_4)} \tag{3}$$

$$D = \frac{j\left(P_4 e^{jkx_3} - P_2 e^{-jkx_4}\right)}{2\sin k(x_3 - x_4)} \tag{4}$$

$$P|_{x=0} = A + B \quad and \quad P|_{x=d} = Ce^{-jkd} - De^{jkd} \tag{5}$$

$$V|_{x=d} = \frac{Ce^{-jkd} - De^{jkd}}{\rho c} \quad and \quad V|_{x=0} = \frac{A+B}{\rho c} \tag{6}$$

$$\binom{P}{V}|_{x=0} = \begin{pmatrix} T_{11} & T_{12} \\ T_{21} & T_{22} \end{pmatrix} \binom{P}{V}|_{x=d} \tag{7}$$

$$\begin{pmatrix} T_{11} & T_{12} \\ T_{21} & T_{22} \end{pmatrix} = \frac{1}{\mathrm{P}|_{x=0} V|_{x=d} + \mathrm{P}|_{x=d}\, V|_{x=0}} \begin{pmatrix} \mathrm{P}|_{x=d} V|_{x=d} + \mathrm{P}|_{x=0}\, V|_{x=0} & \mathrm{P}|^2{}_{x=0} - P|^2{}_{x=d} \\ \mathrm{V}|^2{}_{x=0} - V|^2{}_{x=d} & \mathrm{P}|_{x=d} V|_{x=d} + \mathrm{P}|_{x=0}\, V|_{x=0} \end{pmatrix} \tag{8}$$

$$R = \frac{T_{11} - \rho c T_{21}}{T_{11} + \rho c T_{21}} \tag{9}$$

$$\alpha = 1 - |R|^2 \tag{10}$$

4. Results and Discussion

The coir-based samples in pellet form and mat form are used in this analysis to test the frequency response of their acoustic absorption coefficient. Three coir fiber-based pellets are tested using the impedance tube to measure their passive acoustic absorption. The coir fibers of fiber diameter 120, 180, and 200 µm are used for making the coir pellets of the same thickness. The CCD images of the fibers are shown in Fig. 3. The frequency response of the acoustic absorption coefficient of the three coir pellets is sown in Fig. 4.

Fig. 3. The fiber images of the three different coir fibers used for measurement.

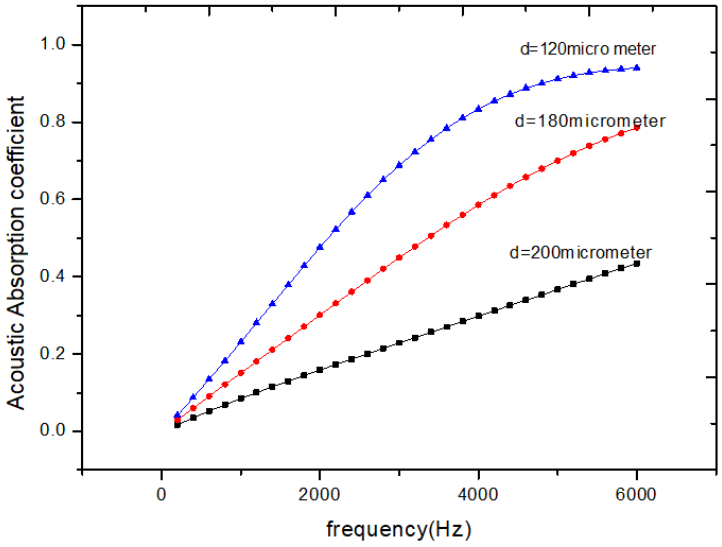

Fig. 4. Frequency response of the acoustic absorption coefficient of the three different samples with different coir fiber diameters.

The frequency response shows that all three samples of different fiber diameters have an inadequate acoustic response in the frequency range below 2000 Hz. According to the theory, the samples show better performance in the entire frequency range when the fiber diameter is decreased [31]. In the sample made of a fiber of 200 µm diameter, the acoustic absorption is deficient. This sample showed poor performance in the entire frequency range with maximum acoustic absorption of 0.4 near the frequency of 6000 Hz. When the fiber diameter decreases to 180 µm, the performance slightly shifts to a higher acoustic absorption range. Out of the three samples, the pellet with the lowest fiber diameter (120 µm) showed the best performance with the acoustic absorption coefficient close to unity in the frequency region between 5000 and 6000 Hz. Thus it is possible to enhance the passive absorption performance of the sample by using coir fibers of lower diameter. The samples are less efficient in the lower frequency region below 2000 Hz.

The frequency response of the acoustic absorption coefficient of coir mats of different weaving patterns is also checked using the impedance tube in the frequency range of 0-6000 Hz in order to understand whether there is any change in acoustic absorption of coir fiber when it is used in this form instead of the pelletized form used earlier. The comparison of the frequency response of the acoustic absorption coefficient of coir mats of two different weaving patterns, namely Panama weaving pattern and Herringbon weaving pattern in the frequency range of 0-6000 Hz, is shown in Fig. 5. In this case, for both the weaving patterns, the maximum acoustic absorption is in the frequency region of 5000-6000 Hz, similar to the coir pellet samples. The graphs indicate that Panama weaved one of lower thickness performs better than the Herringbone weaved one of slightly higher thickness. The frequency response of the acoustic absorption coefficient for the Panama weaved one is compared with that of the Boucle weaved one. The comparison of

the same is shown in Fig. 6. The graph indicates that the best performance is coming in the frequency region between 5000-6000 Hz. The Boucle weaved pattern of lower thickness is the best performing one compared to Panama weaved one and Herringbone weaved patterns of slightly higher thickness. The fiber diameter has a crucial role in determining the airflow resistivity. The fiber with a low diameter has higher airflow resistivity, leading to higher acoustic absorption [31]. The difference in the weaving pattern introduces a difference in porosity, leading to a difference in acoustic absorption, and the samples with high porosity perform better [32].

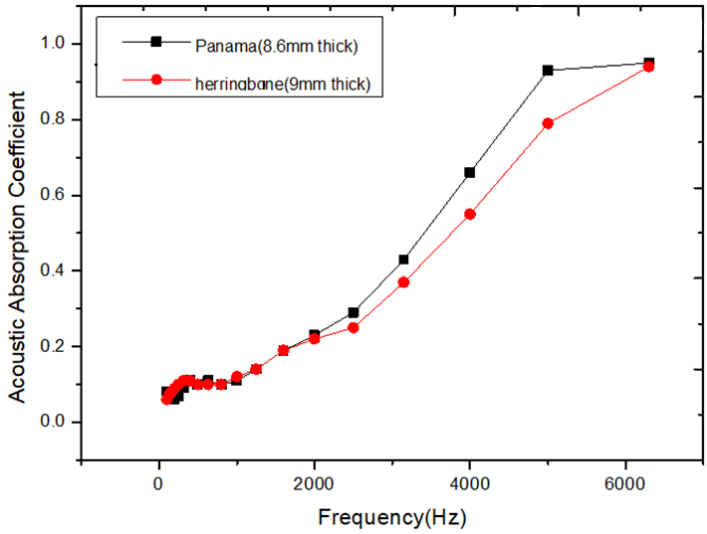

Fig. 5. Comparing the frequency response of the acoustic absorption coefficient of Panama weaved mats and Herringbone weaved ones.

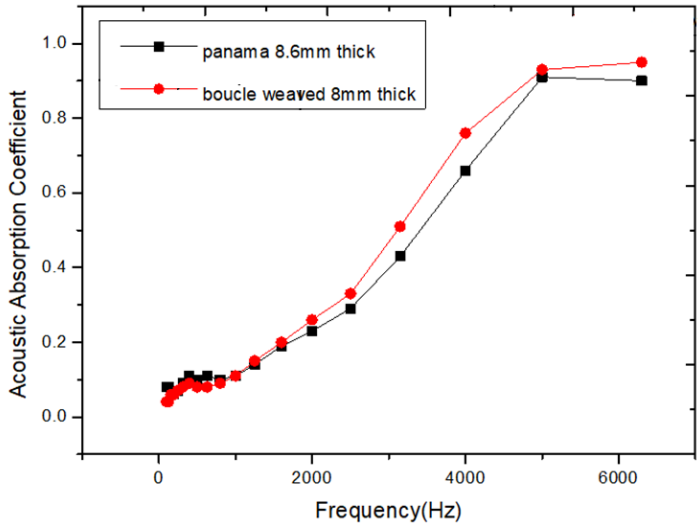

Fig. 6. Comparison of the frequency response of the acoustic absorption coefficient of Panama weaved mats and Boucle weaved ones.

Coir fiber-based samples of two different textures tested perform best in the higher frequency range between 5000-6000 Hz. Their absorption property is weak in the frequency range below 2000 Hz. The glass fiber-based epoxy laminate and basalt fiber-based epoxy laminate are tested for their frequency response of acoustic absorption coefficient in the frequency range below 2000 Hz using a four-microphone impedance tube. The frequency response of the acoustic absorption coefficient in the frequency range 0-2000 Hz is shown in Fig. 7 [33]. The sample shows maximum acoustic absorption of around 0.9 at the frequency range of 1900 Hz. Thus, this sample can be used for passive acoustic absorption in the frequency range below 2000 Hz, where the coir-based ones are proved inefficient. In order to achieve better passive noise controlling, basalt fiber-based epoxy laminate is also tested for its frequency response of acoustic absorption in the frequency range below 2000 Hz. The frequency response of the acoustic absorption coefficient of Basalt fiber-based epoxy laminate is shown in Fig. 8 [33]. The sample shows maximum acoustic absorption of 0.9961 at 1500 Hz. Thus, the low-frequency region below 2000 Hz enhances the maximum absorption compared to the coir fiber-based and glass fiber-based samples. Compared to the glass fiber epoxy laminate, the maximum absorption frequency is lower at 1500 Hz [33]. This sample has a better absorption bandwidth compared to the glass fiber-based epoxy laminate. It can be used as an excellent passive acoustic absorber in the 1400-1600 Hz frequency band. The SEM images of the glass fiber-based and basalt fiber-based samples are shown in Fig. 9 and Fig. 10. The fiber diameters of the glass fiber-based and basalt fiber-based samples are less than the fiber diameters of the coir fibers used in the present study. The SEM image indicates that the fiber diameter of the basalt fiber used is less than that of the glass fiber used for fabricating the epoxy laminate.

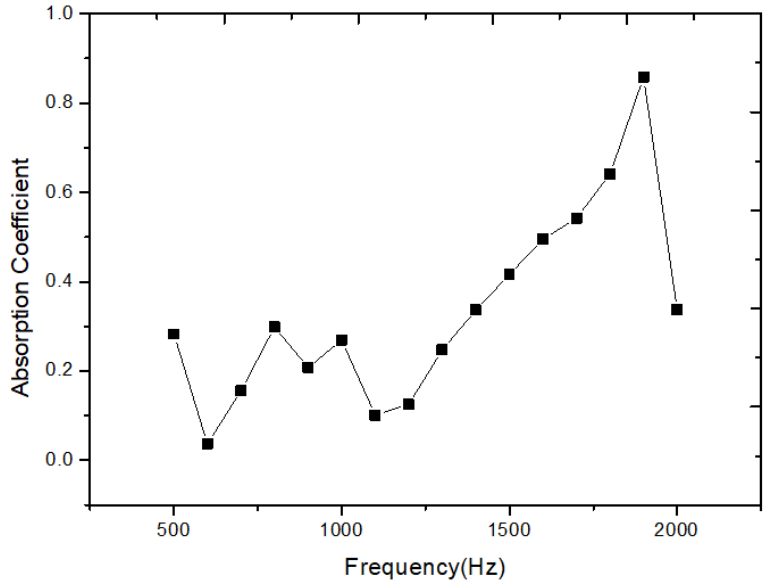

Fig. 7. Frequency response of the acoustic absorption coefficient of glass fiber epoxy laminate.

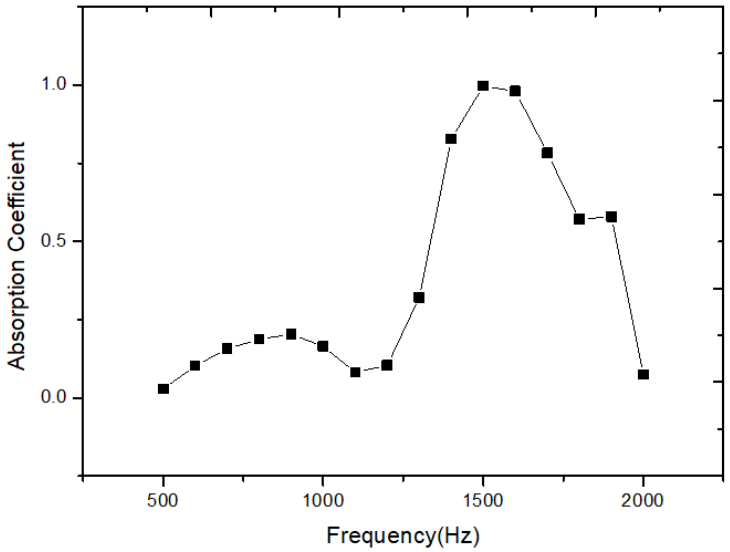

Fig. 8. Frequency response of the acoustic absorption coefficient of basalt fiber epoxy laminate.

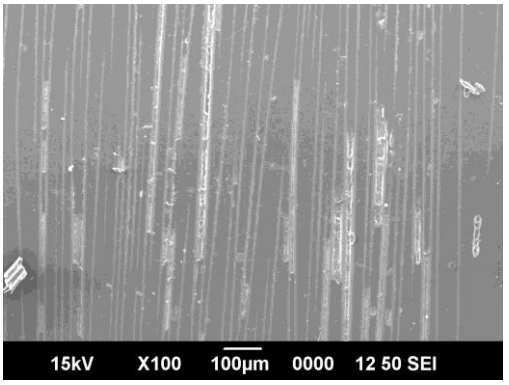

Fig. 9. SEM image of the glass epoxy laminate.

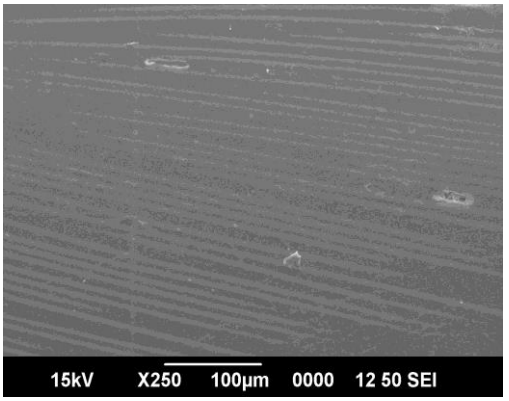

Fig. 10. SEM image of the basalt epoxy laminate.

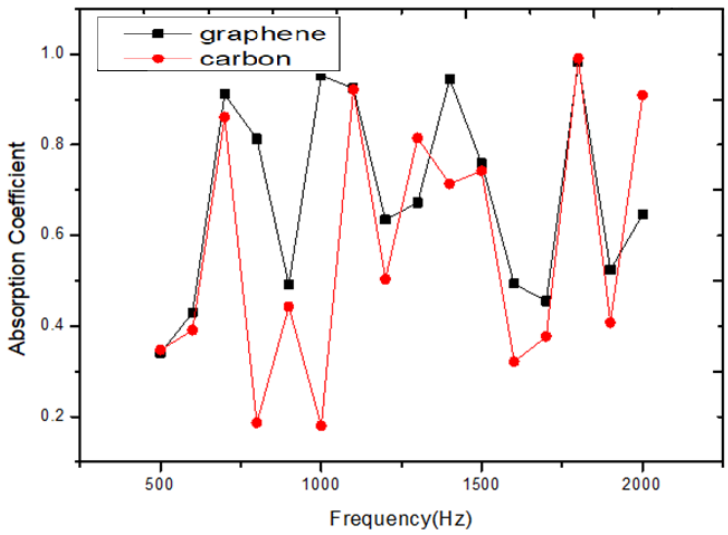

Fig. 11. Comparison of the frequency response of the acoustic absorption coefficient of carbon and graphene epoxy laminate.

The carbon and graphene fiber-based epoxy laminates are tested for the frequency response of their acoustic absorption coefficient. A comparison of the frequency response of the acoustic absorption coefficient of carbon and graphene-based epoxy laminates is shown in Fig. 11. The carbon and graphene-based samples showed maximum acoustic absorption coefficients close to unity at 700, 1100, 1400, 1500, and 1800 Hz in the frequency range of 0-2000 Hz. In this entire band 0-2000 Hz, the graphene sample shows slightly better performance than the another. Both samples showed higher absorption at the lower frequency of 700 Hz in the frequency region close to 500 Hz, where the usual passive absorbers are less efficient than the active ones. So these particular samples can be used as acoustic absorbers in this low-frequency region instead of the active ones. The fiber diameters of the samples are below 50 µm. The fiber diameter and the spacing between the fibers can be seen in the SEM images of these samples. The SEM image of the carbon fiber-based epoxy laminate is shown in Fig. 12, and that of the graphene fiber-based one is shown in Fig. 13. For a better comparison, a single graph shows the absorption characteristics of the four fibrous materials of glass, basalt, carbon, and graphene of the same thickness in Fig. 14 below.

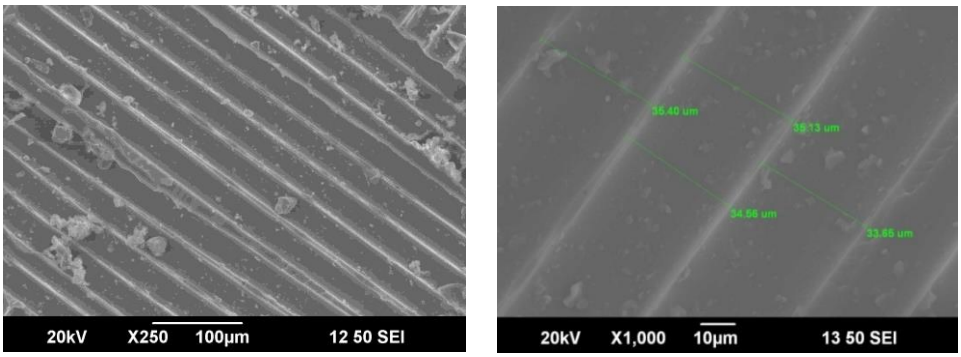

Fig. 12 SEM image of carbon fiber-based epoxy laminate.

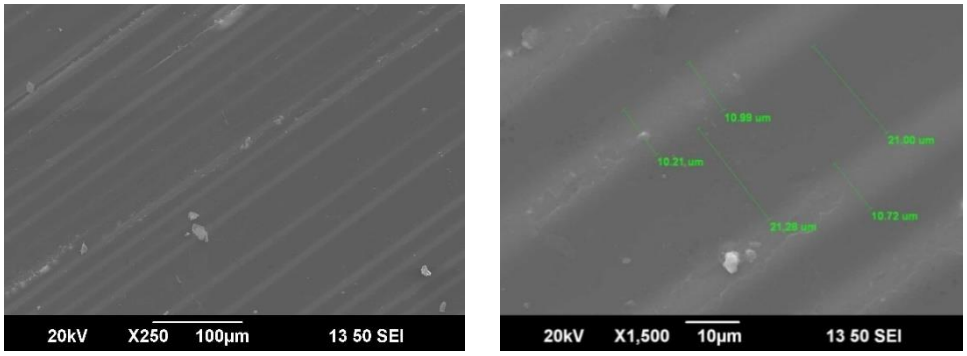

Fig. 13. SEM image of the graphene fiber-based epoxy laminat**e**.

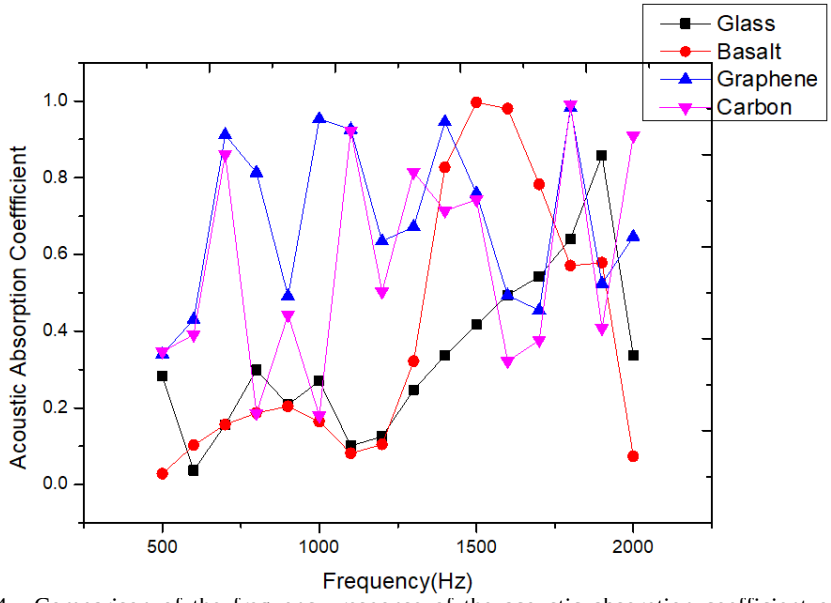

Fig. 14. Comparison of the frequency response of the acoustic absorption coefficient of glass, basalt, carbon, and graphene epoxy laminate.

The moisture-absorbing capability of these natural fiber-based samples decreases its life span compared to synthetic and active noise controllers. The samples' contact angle measurement is also conducted to test the hydrophilic nature cum surface wettability of these samples. Table 1 shows the contact angle measured for these samples. Out of glass fiber epoxy laminate and basalt fiber one, the basalt fiber-based sample is less hydrophilic than the former. The contact angles measurement shows that the graphene-based sample is less hydrophilic than the carbon-based one. The basalt fiber-based sample is least hydrophilic compared to the glass, carbon, and graphene fiber-based samples. By equally considering the lifespan (hydrophilic nature) and the absorption characteristics graphene sample performs better than the other ones in the frequency region below 1000 Hz. Basalt fiber laminate is the better one with a higher life span and acoustic absorption in the frequency region between 1000 and 2000 Hz.

Table 1. The contact angle of the epoxy laminates is under investigation.

Sl. No	Material	Contact angle (deg.)
1	Glass fiber epoxy laminate	51.82
2	Basalt fiber epoxy laminate	55.97
3	Carbon fiber epoxy laminate	44.97
4	Graphene epoxy laminate	47.70

5. Conclusion

Passive noise controllers are proven less efficient in the low-frequency region - significantly below 500 Hz than active ones. Here, different potential natural fiber-based diameter samples in the micrometer range are investigated to achieve low-frequency noise control. All the coir-based samples of different textures used in this study show noise reduction capability in the high-frequency region close to 6000 Hz. The coir samples in pellet form showed maximum sound absorption within the range of 0.9-1.0 in the frequency region 5000-6000 Hz. Out of the coir fibers of three different fiber diameters, 120, 180, and 200 μm tested, the best noise controlling performance is obtained when coir fiber of minimum fiber diameter is used, which agrees with the theory. The airflow resistivity increases when fiber diameter is decreased, leading to higher acoustic absorption. Out of the coir mats of three different weaving patterns, the Boucle weaved pattern showed better performance compared to Panama weaved ones and herringbone ones used in the present study. All three mats have maximum acoustic absorption in the frequency range of 5000-6000 Hz frequency band. Thus weaving pattern has a role in noise controlling as different weaving patterns introduce a difference in the porosity of the sample, and highly porous samples show maximum sound absorption. The glass fiber-based sample has maximum acoustic absorption close to unity near 2000 Hz corresponding to the acoustic frequency at 1900 Hz. In basalt fiber-based samples, the absorption peak is shifted towards the still lower frequency side of 1500 Hz. In the carbon fiber-based sample, three absorption peaks are obtained in the frequency region below 2000 Hz at 700, 1100, and 1800 Hz, and the maximum absorption is obtained at 1800 Hz.

When the graphene-based sample is used, it is possible to enhance the passive absorption better than the carbon fiber-based sample. In this case, peak absorption corresponds to 700, 1000, 1100, and 1800 Hz. In all the cases, the absorption coefficient is slightly higher compared to that of the carbon-based sample. At 700 Hz, an absorption coefficient of 0.91 is obtained for this graphene sample. Thus it is possible to achieve an acoustic absorption coefficient close to unity near 700 Hz for carbon and graphene-based samples, and the performance at 700 Hz is improved when a graphene sample is used. Hence it is clear that the fiber nature, its structural properties, and geometrical properties can be appropriately optimized for utilizing them for passive noise reduction in the low-frequency region below 500 Hz, where active noise controllers are proven as efficient compared to the passive ones. Thus, it is possible to optimize the fiber-based passive noise controllers in the higher frequency range close to 6000 Hz and lower acoustic frequency range below 2000 Hz. The sample's fiber type, diameter, and porosity are essential in determining their acoustic absorption coefficient and frequency response. The contact angle measurement is performed to understand which samples are less hydrophilic to optimize the passive noise controller with a considerable life span.

References

1. E. O. Aluko and V. U. Nna, Victor, Int. J. Trop. Dis. Health **6,** 35 (2015). https://doi.org/10.9734/IJTDH/2015/13791
2. H. P. Kunc, K. E. McLaughlin, and R. Schmidt, Proc. Biol. Sci. **283**, 836 (2016). https://doi.org/10.1098/rspb.2016.0839
3. K. I. Hume, M. Brink, and M. Basner, Noise Health **14**, 297 (2012). https://doi.org/10.4103/1463-1741.104897
4. T. Munzel, T. Gori, W. Babisch, and M. Basner, Eur. Heart J. **35**, 829 (2014). https://doi.org/10.1093/eurheartj/ehu030
5. D. Schreckenberg, B. Griefahn, and M. Meis, Noise Health **12**, 7 (2010). https://doi.org/10.4103/1463-1741.59995
6. D. J. Oxley, M. B. Fenton, and G. R. Carmody, J. Appl. Ecol. **11**, 51 (1974). https://doi.org/10.2307/2402004
7. S. C. Trombulak and C. A. Frissell, Conserv. Biol. **14**, 18 (2000). https://doi.org/10.1046/j.1523-1739.2000.99084.x
8. L. Andren, Acta Med. Scand. Suppl, **657**, 1 (1982).
9. L. Andren, L. Hansson, R. Eggertsen, T. Hedner, and B. E. Karlberg, Acta Med. Scand. **213**, 31 (1983). https://doi.org/10.1111/j.0954-6820.1983.tb03685.x
10. T. Lang, C. Fouriaud, and M. C. Jacquinet-Salord, Int. Arch. Occup. Environ. Heath **63**, 369 (1992). https://doi.org/10.1007/BF00386929
11. N. Broner, J. Sound Vibr. **58**, 483 (1978). https://doi.org/10.1016/0022-460X(78)90354-1
12. R. I. Henkin and K. M. Knigge, Am. J. Physiol. **204**, 710 (1963). https://doi.org/10.1152/ajplegacy.1963.204.4.710
13. K. Iwai, S. Hase, and Y. Kajikawa, Appl. Sci. **8**, 2291 (2018). https://doi.org/10.3390/app8112291
14. M. Pawelczyk, Adv. Acoustics Vibr. **2008**, 350943 (2008). https://doi.org/10.1155/2008/350943
15. S. Wise and G. Leventhall, J. Low Frequency Noise, Vibr. Active Control **29**, 129 (2010). https://doi.org/10.1260/0263-0923.29.2.129
16. X. Sagartzazu, L. Hervella-Nieto, and J. M. Pagalday, Archiv. Comput. Methods Eng. **15**, 311 (2007). https://doi.org/10.1007/s11831-008-9022-1

17. R. R. Koireng, P. C. Agarwal, and A. Gokhroo, J. Sci. Res. **13**, 21(2021). https://doi.org/10.3329/jsr.v13i1.47327
18. H. S. Seddeq, Aust. J. Basic Appl. Sci. **3**, 4610 (2009).
19. R. D. Ford, and M. A. McCormick, J. Sound Vibr. **1969**, 41l (1969).
20. Y. Lu, H. Tang, J. Tian, and Hongqi Li, J. Acoust. Soc. Am. **119**, 324 (2006). https://doi.org/10.1121/1.4785889
21. J. P. Arenas and Ma. J. Crocker, Sound Vibr., Mater. **13**, 12 (2010).
22. U. Kalita, A. Pratap, and S. Kumar, Int. J. Mech. Ind. Technol. **2**, 31 (2015).
23. N. Atalla and R. Panneton, J. Sound Vibr. **243**, 659 (2001). https://doi.org/10.1006/jsvi.2000.3435
24. S. Huang, X. Fang, X. Wang, B. Assouar, Q. Cheng, Y. Li, J. Acoust. Soc. Am. **145**, 2549 (2019). https://doi.org/10.1121/1.5101806
25. D. C. Brooke, O. Umnova, P. Leclaire, and T. Dupont, J. Sound Vibr. **485**, 1 (2020). https://doi.org/10.1016/j.jsv.2020.115585
26. S. Rajappan, P. Bhaskaran, and P. Ravindran, J. Appl. Sci. **17**, 339 (2017). https://doi.org/10.3923/jas.2017.339.356
27. D.-Y. Maa, J. Acoust. Soc. Am. **104**, 2861 (1998). https://doi.org/10.1121/1.423870
28. J. S. Hayward and B. Harris, Compos. Manufacturing **1**, 161 (1990). https://doi.org/10.1016/0956-7143(90)90163-Q
29. Y. Takahashi, T. Otsuru, and R. Tomiku, Appl. Acoust. **66**, 845 (2005). https://doi.org/10.1016/j.apacoust.2004.11.004
30. J. Y. Chungand and D. A. Blaser, J. Acoust. Soc. Am. **68**, 907 (1980). https://doi.org/10.1121/1.384778
31. M. E. Delany and E. N. Bazley, Appl. Acoust. **3**, 105 (1970). https://doi.org/10.1016/0003-682X(70)90031-9
32. X. Luo, W. Li, X. Jin, and L. Zeng, J. Chin Ceram. Soc. **39**, 159 (2011).
33. S. Rajappan, P. Bhaskaran, and M. S. Roxy, J. Ultra Scientist Phy. Sci. Section B **30**, 72 (2018). https://doi.org/10.22147/jusps-B/300701